A Model-Free ON–OFF Iterative Adaptive Controller Based on Stochastic Approximation

Bongsu Hahn and and Kenn R. Oldham, *Member, IEEE*

***Abstract*—A model-free ON–OFF iterative adaptive controller is described for application to microscale servo systems performing repeated motions under extremely strict power constraints. The approach is motivated by the needs of piezoelectric actuators in autonomous microrobots, where power consumption in analog circuitry and/or for position sensing may be much larger than that of the actuators themselves. The control algorithm adjusts switching instances between "ON" and "OFF" inputs to the actuator to minimize an objective function using simultaneously perturbed stochastic approximation of the gradient with just a single sensor measurement in each iteration. Convergence conditions for the gradient approximation are shown to apply when the possibility for a range of possible switching times minimizing the objective function is accounted for, while a method is proposed for avoiding local minima for plants with bounded nonlinearities. The algorithm is tested on a prototype piezoelectric microactuator.**

***Index Terms*—Adaptive control, gradient approximation, iterative control, microelectromechanical systems (MEMS), microrobotics, model free, ON–OFF control, piezoelectric actuation, piezoelectric actuators.**

I. Introduction

MINIATURIZATION of sensors and actuators through developments in microelectromechanical systems (MEMS) technology can enable very low-power, small footprint implementation of a variety of engineered systems. Piezoelectric and electrostatic actuators are two of the most common mechanisms for generating motion in MEMS devices and act as capacitive loads with very small intrinsic power consumption. For instance, a 1 nF piezoelectric actuator operating at 20 V and 20 Hz requires less than 10 μW of power. However, unknown and/or nonlinear behavior may require feedback control, in which case actuator power consumption can be exceeded by that of drive and sensing circuitry.

To achieve low power consumption of a complete servo control system for microscale piezoelectric or capacitive actuators, it is desirable to utilize switching ("ON–OFF") control to avoid inefficiencies in driving circuits [1] as well as to minimize the number of times that the circuit switches during a given controlled motion. For well-known system dynamics, sensing may be omitted and open-loop input sequences used [3], [4], [7], including for open-loop energy minimization [29].

On the other hand, when dynamics are unknown, difficult to model, or varying, it is necessary to implement a feedback control system that is robust or can adapt the switching sequence applied to the system using feedback. Reducing the number of sensor measurements taken can reduce system power consumption significantly because sensing circuit power typically rises with sampling rate. For example, one sample ultralow-power capacitive sensing circuit requires not more than 10 μW at low duty cycles (sampling rate <25 Hz), but almost 100 μW at full operation approaching 250 Hz [2].

This paper examines an iterative controller for an "ON–OFF" switching control system, in which a desired motion is to be completed many times with the ability to adjust the input sequence between movements. Motivating this study is the walking gait of a piezoelectrically driven microrobot, whose legs may need to complete the same stepping motion a large number of times under an extremely constrained power budget. Fig. 1 shows concept drawing of a bio-inspired terrestrial microrobot design and image of a prototype piezoelectric leg joint. The weight-bearing capacity of such a robot is anticipated to be in the range of 5–50 mg [5], corresponding to an available power consumption per leg of approximately 100–700 μW based on state-of-the-art thin-film batteries or solar cells [6] such that sensor power, and hence, sampling rate, has a significant effect on power allocation.

To perform low-power servo control, the problem of selecting transition times of an ON–OFF input sequence is converted to a model-free adaptive control problem with the adaptive controller based on the simultaneous perturbation stochastic approximation (SPSA) developed by Spall [10]–[13]. This controller has several benefits for power minimization in microrobotics, including a need for only one sensor measurement each time an individual actuator [such as one of the joints in Fig. 1(b)] moves through a desired motion, the ability to perform computation between steps to reduce processor requirements, and

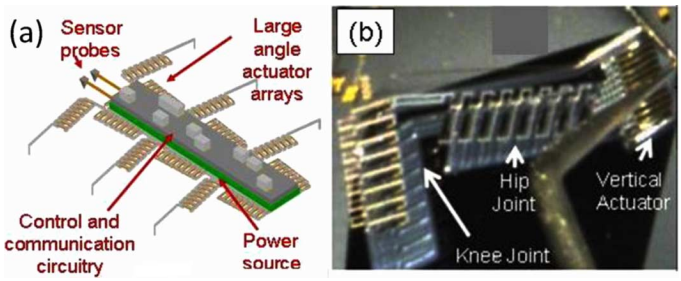

Fig. 1. (a) Concept drawing of an autonomous microrobot. (b) Prototype microrobotic leg joint. Courtesy: U.S. Army Research Laboratory.

Manuscript received July 16, 2010; revised October 15, 2010; accepted November 25, 2010. Manuscript received in final form December 31, 2010. Date of publication February 10, 2011; date of current version December 14, 2011. Recommended by Associate Editor A. Alessandri. This work was supported in part by the U.S. Department of Defense under Grant W911QX-07-C-0072 and Grant HR0011-08-1-0040.

The authors are with the Department of Mechanical Engineering, University of Michigan, Ann Arbor, MI 48109 USA (e-mail: suhahn@umich.edu; oldham@umich.edu).

Color versions of one or more of the figures in this paper are available online at http://ieeexplore.ieee.org.

Digital Object Identifier 10.1109/TCST.2011.2104360

effectiveness in the presence of noisy sensors. A model-free approach was selected because the piezoelectric actuators targeted are nonlinear [19], and uncertainty in system properties is anticipated due to the varying environments that such a microrobot might encounter.

The proposed algorithm differs from previous adaptive switching controllers in being both model free and relying on a very limited number of sensor measurements. Previous controllers oriented toward ON–OFF control, as well as most other adaptive switching controllers, have relied on model-based adaptation [20], [21]. Other model-free adaptive controllers have typically been organized around neural nets, which have not yet been applied to ON–OFF control problems; a neural net approach could potentially perform function estimation in the ON–OFF context as well, though the assumption of an affine dependence on input in most cases prevents existing algorithms from being directly applicable [22]–[24] when switching time is the input being adapted.

In addition to formulating the adaptive ON–OFF control problem in a manner compatible with stochastic approximation, this paper provides a minor extension of SPSA convergence analysis for regions of local minima, rather than just single points, and tests the algorithm experimentally on a prototype microrobotic leg joint. In addition, an approach is provided to select initial switch times and adaptation targets to avoid local, rather than global, minima in cases of short duration motions with bounded, unknown nonlinearities.

II. System Description

The dynamic system to be considered consists of a state vector $\boldsymbol{x} \in \boldsymbol{R}^N$ and input $\boldsymbol{u} \in \boldsymbol{R}$, and a set of unknown, differentiable, Lipschitz continuous, and possibly nonlinear state and input equations $\boldsymbol{f}(\boldsymbol{x})$ and $\boldsymbol{v}(\boldsymbol{x})$. In the case of ON–OFF control with only two possible inputs $\boldsymbol{u} \in \{0, u_{\max}\}$, two alternate functions may be used to define dynamics $\boldsymbol{l_1}(\cdot)$ for the "ON" state ($u = u_{\max}$) and $\boldsymbol{l_0}(\cdot)$ for the OFF state ($u = 0$). There is a known, linear relationship between states and a measured variable $y \in \boldsymbol{R}$ defined by matrix $\mathbf{C}$, giving system dynamics

$$\begin{aligned}\dot{\boldsymbol{x}}(t) &= f(\boldsymbol{x}(t)) + \nu(\boldsymbol{x}(t))u(t) \\ &= \begin{cases} l_0(\boldsymbol{x}(t)), & u(t) = 0 \\ l_1(\boldsymbol{x}(t)), & u(t) = u_{\max} \end{cases} \\ y(t) &= \mathbf{C}\boldsymbol{x}(t) + \varepsilon(t) \end{aligned} \tag{1}$$

where $\varepsilon(t)$ is white, Gaussian, zero-mean measurement noise.

The system in (1) is taken to be asymptotically stable, with "ON" and "OFF" equilibrium points $\boldsymbol{r}_0$ and $\mathbf{0}$, satisfying

$$\begin{cases} \boldsymbol{l_1}[\boldsymbol{x}(t)] = \mathbf{0}, & \text{iff } \boldsymbol{x} = [\, r_0 \quad 0 \quad \ldots \quad 0\,] \\ \boldsymbol{l_0}[\boldsymbol{x}(t)] = \mathbf{0}, & \text{iff } \boldsymbol{x} = \mathbf{0}. \end{cases} \tag{2}$$

A response of time duration t_f is to be produced many times, with the state, measurement, and input vectors from the kth iteration are denoted by $\boldsymbol{x}^k, y^k$, and u^k, respectively. We assume that the (1) have a real, unknown solution $\psi(\cdot)$, which can also be written as a solution $\psi_0(\cdot)$ or $\psi_1(\cdot)$ for inputs in the "OFF" or "ON" state, respectively

$$\begin{aligned}\boldsymbol{x}^k(t) &= \psi(t - t_0, \boldsymbol{x}^k(t_0), u^k(t)) \\ &= \begin{cases} \psi_0(t - t_0, \boldsymbol{x}^k(t_0)), & u(t) = 0 \; \forall t > t_0 \\ \psi_1(t - t_1, \boldsymbol{x}^k(t_0)), & u(t) = u_{\max} \; \forall t > t_0 \end{cases} \end{aligned} \tag{3}$$

In addition, we assume that there is sufficient time between iterations to treat

$$\boldsymbol{x}^k(0) = \mathbf{0} \tag{4}$$

for all iterations k due to the stability of the system with zero input and an assumption of satisfactory time between motions for the system to return to its "OFF" equilibrium state.

The model described in (1)–(4) provides a good representation of the piezoelectric actuators motivating this project among other dynamic systems. The piezoelectric actuators consist of continuous flexible structures with differentiable behavior in mechanical dynamics and piezoelectric response. The system inputs are limited to "ON" and "OFF" voltages supplied by an ultralow-power switching circuit. While the piezoelectric actuation gain, structural stiffness, and damping effects may be nonlinear functions of system states, equilibrium positions at voltages of 0 and $u_{\max}$ exist and are easily measured. Finally, we anticipate there being sufficient time (for example, while other legs are propelling the robot body) for individual actuators to return to their original position before being actuated again, and experimental testing indicates that the high stiffness of silicon flexures in comparison to the piezoelectric materials results in negligible variation in initial conditions due to any hysteresis in the piezoelectric response [29]. In addition, despite hysteresis, actuator gains alternate between consistent levels as each input is always reached from the same previous voltage level.

III. Control Problem

The control objective is to drive the true output of the system at a specified final time $y(t) = \mathbf{C}\boldsymbol{x}(t)$ to a desired target value r over several iterations of motion. The control input in each iteration is a real, bounded function $h(\cdot)$ of a parameter vector θ^k. In the general control input case with continuous inputs $u^k \in \boldsymbol{R}$, this results in an iterative system input described by

$$u^k = h(\theta^k), \qquad \theta^k = [\, \theta_1^k, \quad \theta_2^k, \quad \ldots, \quad \theta_p^k \,]. \tag{5}$$

The control system goal becomes to find an optimized parameter vector set θ^k minimizing the error between the system output and reference under a fixed power consumption with fixed ON–OFF transitions rather than a full minimization of power output feedback, which is assumed to be made sufficiently low by using a small number of switching transitions and sensor measurements. The ideal minimization problem with respect to θ^k and output error can then be stated as follows:

$$\min_{\theta_i^k \geq 0, i=1,\ldots,p} \left(J(\theta^k) = \frac{1}{2} \int_0^{t_f} (\mathbf{C}\boldsymbol{x}(t) - r)^2 dt \right). \tag{6}$$

To solve problem (6), typically a gradient-based optimization method is used, as in the following:

$$\theta^{k+1} = \theta^k - \alpha^k \boldsymbol{g}(\theta^k)$$
$$\boldsymbol{g}(\theta^k) = \left(\frac{\partial \boldsymbol{x}}{\partial \theta^k}\right)^T \left(\frac{\partial J}{\partial \boldsymbol{x}}\right)^T \tag{7}$$

where α^k is the step size of the algorithm, and $\boldsymbol{g}(\theta^k)$ is the p-dimensional gradient vector for the cost function $J(\cdot)$ with respect to θ^k. This approach is used by several model-based controllers [3], [7], [8], [9]. In these controllers, the system dynamics function $\psi(\cdot)$ is completely known and there is no consideration of minimal use of measurement outputs. However, the gradient in (7) for the cost function cannot be determined in this paper because it is assumed that (6) and (7) are based on unknown functions $\psi(\cdot)$, $f(\cdot)$, and $v(\cdot)$. Additionally, reduction of measurements is not accounted for by the standard gradient approaches because the gradient is based on derivation of a complete function. Even though a tradition gradient approximation, finite difference stochastic approximation (FDSA), is not based on a complete function, FDSA should account many measurements; SPSA uses p times fewer gradient evaluations than FDSA [11].

To solve this problem, the SPSA algorithm is used for gradient approximation in this paper. This approximation method was developed by previous researchers as a model-free approach for finding optimal control parameters [15]–[18]. SPSA is based on relating random perturbations of controller parameters with their influence on a cost function, which is in turn a function of output measurements from an unknown system with random noise. Thus, SPSA does not require full knowledge of the form of the system dynamics. Most importantly, since SPSA requires only one or two measurements to compute gradient approximations, regardless of the dimension, such as the problem (7), it is very useful and effective for limited measured outputs. Previous controllers based on SPSA have utilized a fixed functional structure for a controller, such as a neural network or a polynomial, which generates analog inputs. In contrast, an ON–OFF controller permits only two possible input states, and this behavior must be defined in a way that is compatible with the SPSA algorithm.

IV. Model-Free ON–OFF Control Algorithm

In this section, we define the controller parameters, a cost function, and a parameter-updating rule for a model-free iterative adaptive approach to control. Properties of the system under ON–OFF control will be related to convergence conditions of the one-measurement form of the SPSA (as provided in [10] and [12]). Fig. 2 shows the block diagram of the iterative adaptive ON–OFF controller using the SPSA algorithm.

A. Adaptive ON–OFF Controller

For a single-measurement scenario, the control task is to steer the true output of the system at the final time $y_f^k = \mathbf{C}\boldsymbol{x}(t_f)$ to a desired target r by finite-time ON–OFF control using p switching instances and a single measurement output. Under finite-time ON–OFF control, the input u^k applied to the system (1) varies

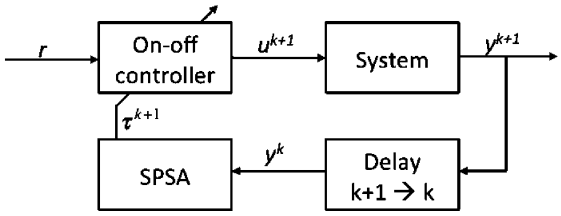

Fig. 2. Block diagram of the controller.

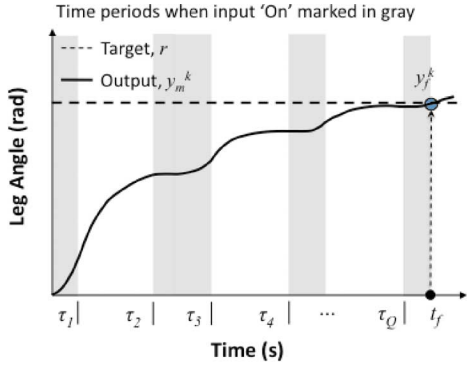

Fig. 3. Illustration of input time parameter definitions.

switching times while alternating between zero and a constant maximum value $u_{\max}$.

Switching times are defined by the final time t_f and time vector $\tau^k \in \boldsymbol{R}^p$, with the system output (5) being rewritten as a function of τ^k, giving

$$\tau^k = [\tau_1^k, \quad \tau_2^k, \quad \ldots, \quad \tau_p^k] \tag{8}$$
$$y_f^k = \mathbf{C}\psi(t_f, 0, h(\tau^k)). \tag{9}$$

As shown in Fig. 3, in this formulation, the time periods between switching instances τ^k serve as the parameter vector θ^k in (5), and therefore, the relationship $h(\cdot)$ between parameters and input u^k may be described for $r = 1, 2, \ldots, (p/2)$ by

$$\begin{aligned} u^k &= u_{\max}, \qquad \text{for } \tau_{2r-1}^k \le t < \tau_{2r}^k \\ u^k &= 0, \qquad \text{for } \tau_{2r}^k \le t < \tau_{2r+1}^k \\ u^k &= 0, \qquad \text{for } \tau_p^k \le t \le t_f. \end{aligned} \tag{10}$$

Since only one measurement output will be used

$$\min_{\tau_1 \ge 0, \tau_i \le \tau_{i+1}, \tau_p \le t_f} \left(J(\tau^k) = \frac{1}{2}\left(y_f^k - r\right)^2 \right) \tag{11}$$

replaces the minimization problem (6). By the SPSA algorithm, the problem defined in (11) may be solved by updating the input parameter vector τ^k until the cost function $J(\cdot)$ goes to zero as the iterative index k goes to infinity.

B. Iterative Update of τ^k Using SPSA Algorithm

The one-measurement form of the SPSA algorithm [12] for the control problem defined in (11) is applied to the switching control problem as follows.

Let $\hat{\tau}^k$ be the estimate of τ^k at the iteration k. SPSA has the standard iterative form

$$\begin{aligned}\hat{\tau}^{k+1} &= \hat{\tau}^k - a^k \hat{g}^k(\hat{\tau}^k) \\ a^k &= \frac{a}{(k+A)^\alpha}\end{aligned} \tag{12}$$

where a^k is a sequential gain coefficient, and $\hat{g}^k(\hat{\tau}^k)$ is a simultaneous perturbation (SP) approximation to the unknown gradient vector $\boldsymbol{g}(\cdot)$ for the cost function $J(\cdot)$ with respect to τ^k at the kth iteration.

The one-measurement SPSA form of the $\boldsymbol{g}(\cdot)$ estimation at iteration k is

$$\begin{aligned}\hat{g}^k(\hat{\tau}^k) &= \frac{Y^{(+)k}}{c^k}\left[1/\Delta_1^k, \quad 1/\Delta_2^k, \quad \ldots, \quad 1/\Delta_p^k\right]^T \\ c^k &= \frac{c}{k^\gamma}\end{aligned} \tag{13}$$

where $\{\Delta^k \in R^N | \Delta^k = [\Delta_1^k, \quad \Delta_2^k, \quad \ldots, \quad \Delta_p^k]^T\}$ is a vector of p independent zero-mean random variables, c^k is a sequential gain, and $Y^{(+)k}$ is the measured cost function value with the control parameter's random perturbation vector Δ^k, and the noise isolated as $\tilde{\varepsilon}^k$, i.e.,

$$Y^{(+)k} = J(\hat{\tau}^k + c^k \Delta^k) + \tilde{\varepsilon}^k. \tag{14}$$

Note that only one measurement is required to form the gradient estimation at each iteration.

C. Implementation of an Adaptive ON–OFF Controller

The iterative ON–OFF time-optimized control for the system (9) can be determined by using the method described in Section IV-A–B with the following procedure.

Step 1) Pick initial guesses for p, t_f, τ^0.

Step 2) Select coefficients, α, γ, A, c, and a.
Recommended values for α and γ are 0.602 and 0.101, respectively, as established in [13]. Effective c can be equal to or less than the estimated standard deviation of the measurement noise. The value of A is selected by a 10% (or less) value of the maximum number of expected/allowed iterations. Choose a such that (15) holds as follows:

$$\begin{aligned}&\frac{a}{(k+A)^\alpha} \times \text{magnitude}[\hat{g}^0(\hat{\tau}^0)] \\ &\quad = \text{smallest desired magnitude change}, \\ &\qquad\qquad k = 0, \ldots, 1.\end{aligned} \tag{15}$$

For detail of theoretical validation and practical effectiveness, see [13] and [28].

Step 3) Generate the SP vector $\boldsymbol{\Delta}^k$.
One of the candidates for the perturbation, and used in this paper, is a symmetric Bernoulli ± 1 distribution with a probability of 1/2 [14].

Step 4) Generate u^k from $\tau = \hat{\tau}^k + c^k \boldsymbol{\Delta}^k$ by and (10).

Step 5) Measure system output at final time t_f.

Step 6) Evaluate the cost function (14).

Step 7) Approximate the gradient by (13).

Step 8) Update τ estimate (12) and check constraint (16); the ability to utilize constraints in the SPSA algorithm, having been shown in [27], is as follows:

$$\text{Constraint}: \begin{array}{ll}\hat{\tau}^k \in [0, \tau^1], & \text{for } y_f^1 > r \\ \hat{\tau}^k \geq 0, & \text{for } y_f^1 \leq r\end{array}. \tag{16}$$

Step 9) Go to Step 3 or terminate algorithm if τ^k is smaller than a prespecified bound or a maximum allowed number of iterations has been reached, subject to available memory.

This implementation satisfies convergence conditions to reach a minimum of the objective function in (11) almost surely, as discussed in more detail in the following. Section V of this paper describes steps that may be taken in some cases to ensure that y_f^k converges to the target r as $k \to \infty$, not just a local minima.

D. Note for Convergence of the Proposed Algorithm

The specified properties of the dynamic system to be controlled and implementation of the adaptive ON–OFF controller based on SPSA are necessary so that an approximated $\hat{\tau}^k$ converges to a minimizing point τ^*. These conditions are related to properties of gain sequences, iterate boundedness, measurement noise, smoothness of a cost function in its relation to system ordinary differential equations (ODEs) , and statistical properties of the perturbations. Under them, the following Proposition 1 can be true.

Proposition 1: If convergence conditions related to SPSA hold and there exists an optimal τ^* for which τ^0 lies within the domain of attraction, then $\hat{\tau}^k \to \tau^*$ as $k \to \infty$ almost surely, or

$$p\left(\lim_{k\to\infty} \hat{\tau}^k \to \tau^*\right) = 1 \tag{17}$$

where τ^* is a minimum of (11).

For detailed properties of the conditions and theoretical proof of Proposition 1 for the general SPSA algorithm, see [10] and [12].

When applying the SPSA algorithm to ON–OFF control, it is important to confirm that the properties target plant subject to ON–OFF control can satisfy properties of convergence conditions of SPSA. First, for an ON–OFF controller driving a system with continuous, differentiable dynamics, the finite duration t_f and finite input magnitude $u_{\max}$ of the ON–OFF controller ensure that the system output measurement y_f control parameters in τ, and cost function $J(\cdot)$ will be bounded. This ensures that properties of iterative boundedness are satisfied. Second, following Steps 2 and 3 during implementation ensures that required properties of gain sequences and statistical properties of the perturbations are met. Third, since the source of noise in the system is taken to be white, Gaussian noise in sensor measurements independent of noise during prior steps and internal computations, properties of measurement noise can be satisfied. Finally, it was assumed that the system plant (1) satisfied Lipschitz continuity. This ensures that the cost function $J(\cdot)$ is three times differentiable, and that the properties of smoothness can be satisfied.

In the nominal SPSA algorithm, Proposition 1 implies almost sure convergence to the local minimum corresponding to an initial choice of τ when convergence conditions are satisfied. For a specific minimizing solution to a cost function, as in (11), the deterministic form and conceptual solution set of (12) can be related as an ODE as k goes to infinity [25], [26] as follows:

$$\frac{d\tau}{dt} = -\boldsymbol{g}(\tau) \tag{18}$$

$$\boldsymbol{D}(\tau^*) = \{\tau^0 \mid \lim_{t\to\infty} \tau(t \mid \tau^0) = \tau^*\} \tag{19}$$

where $g(\tau)$ is a continuous function on $\boldsymbol{R}^p$, τ^* is an asymptotically stable solution of (18), $\boldsymbol{D}^*(\cdot)$ is the domain of convergence, and $\tau(t \mid \tau^0)$ is the solution of (18) with initial condition τ^0 .

For the proposed ON–OFF control using the SPSA algorithm, minima may exist, where $\partial J^k/\partial \tau^k = 0$, which may occur if $y_f^k = r$ (as desired) or $\partial y_f^k/\partial \tau^k = 0$ (a local minima), as seen in the derivative of the cost function

$$\frac{\partial J^k}{\partial \tau^k} = \left(\frac{\partial y_f^k}{\partial \tau^k}\right)^T \left(\frac{\partial J^k}{\partial y_f^k}\right)^T = \left(\frac{\partial y_f^k}{\partial \tau^k}\right)^T \left(y_f^k - r\right). \tag{20}$$

In the case of ON–OFF control, and differing from prior control examples done using the SPSA algorithm, at the minima when $y_f^k = r$, there may exist several, continuous solutions $\tau^* \in \Theta^*$, which can drive system (9) to target r , where Θ^* is a solution set of (12) such that an adjustment to standard SPSA convergence conditions is necessary.

To do so, define a new parameter vector such that $\bar{\tau}^k \equiv ||\tau^k - \tau^*||$, where τ^* is now the set of minima. Then, (18) and (19) can be restated as follows:

$$\frac{d\bar{\tau}}{dt} = -\boldsymbol{g}(\bar{\tau}) \tag{21}$$

$$\boldsymbol{D}(\bar{\tau}^*) = \{\bar{\tau}^0 \mid \lim_{t\to\infty} \bar{\tau}(t \mid \bar{\tau}^0) = \bar{\tau}^*\}. \tag{22}$$

Properties of iterate boundedness and smoothness of a cost function by $\bar{\tau}^k$ remain satisfied by properties of a system subject to ON–OFF control, as described by (21) and (22).

Proposition 2: Supposing standard convergence conditions of the SPSA hold, (21) and (22) hold, if the assumptions A-1 and A-2 are satisfied, then from the extended global Kushner–Clark theorem [25]

$$\bar{\tau}^k \to 0 \quad \text{as } k \to \infty.$$

A-1) $\|b_k(\bar{\tau}^k)\| < \infty$, for a k and $b_k(\bar{\tau}^k) \to 0$, almost surely;
A-2) $\lim_{k\to\infty} P(\sup_{m\geq k} \|\sum_{i=k}^m a_i e_i(\bar{\tau}^k)\| \geq \eta) = 0$, for any $\eta > 0$;

where $b_k(\cdot)$ is the bias between a gradient estimator and the real gradient, $b_k(\bar{\tau}^k) \equiv E(\hat{g}^k(\bar{\tau}^k) - g(\bar{\tau}^k) \mid \bar{\tau}^k)$, $e_k(\cdot)$ is the error in the gradient estimate, $e_k(\bar{\tau}^k) \equiv \hat{g}^k(\bar{\tau}^k) - E(g(\bar{\tau}^k) \mid \bar{\tau}^k)$, and a_i is the gain sequence from (12) . For Proof of Proposition 2 given as A-1 and A-2, see [25], while A-1 and A-2 are used for derivation of the SPSA in [10] and [12].

By Propositions 1 and 2, it may be concluded that the proposed adaptive ON–OFF controller will almost surely converge to a minima of the cost function associated with the initial control parameters provided to the system.

V. Local Minima for Bounded Uncertainty

The convergence analysis in Section IV ensures almost certain (probability $= 1$) convergence of switching times to a solution minimizing (11), but does not yet distinguish between global minima and local minima or indicate how to select initial guesses τ_0 to reach a specified y_f. For general nonlinear functions, there is no known method for ensuring convergence to a global minimum. When dynamics are known, Kaya and Noakes suggest a method for selecting future initial guesses based on past results [3], while for unknown dynamics, some bounds on the nonlinear dynamics are required, as in [21].

For ON–OFF control over short time duration with known bounds on maximum nonlinearity magnitudes, it can be possible to identify values for τ that may result in local minima, and select the target output r and initial guess to avoid them. We note from (20) that a minimum may exist, where $y_f = r$ (desired), or where $\partial y_f/\partial \tau_i = 0$ for all i (undesired). For ON–OFF control, y_f and its partial derivatives with respect to switching times are

$$y_f = \mathbf{C}\psi_0(t_f - \tau_p, \psi_1(\tau_p - \tau_{p-1}, \psi_0(\ldots, \psi_1(\tau_1, \mathbf{0})))) \tag{23}$$

$$\frac{\partial y_f}{\partial \tau_p} = \boldsymbol{C}\left[-\boldsymbol{l}_0(\boldsymbol{x}(t_f)) + \left.\frac{\partial \psi_0}{\partial \boldsymbol{x}(0)}\right|_{t_f-\tau_p} \boldsymbol{l}_1(\boldsymbol{x}(\tau_p))\right]$$

$$\vdots$$

$$\frac{\partial y_f}{\partial \tau_1} = \boldsymbol{C}\left.\frac{\partial \psi_0}{\partial \boldsymbol{x}(0)}\right|_{t_f-\tau_p} \left.\frac{\partial \psi_1}{\partial \boldsymbol{x}(0)}\right|_{\tau_p-\tau_{p-1}} \cdots \left.\frac{\partial \psi_0}{\partial \boldsymbol{x}(0)}\right|_{\tau_2-\tau_1} \times [\boldsymbol{l}_1(\boldsymbol{x}(\tau_1))]. \tag{24}$$

While the functions $\boldsymbol{l_0}, \mathbf{l_1}, \psi_\mathbf{0}$, and $\psi_\mathbf{1}$, and their derivatives in (23) are unknown, if bounds are placed on the difference between the nonlinear system and a known dynamic system, the possible range of the partial derivative terms $\partial y_f/\partial \tau_i$ may be obtained through the use of Gronwall's inequality [30]. The error bounds between the known system's response and the actual unknown system's response grow rapidly with time. However, for short time durations, as in the case of repeated stepping motions desired for the motivating example, it can be possible to identify ranges of values for switching time vector τ, where $\partial y_f/\partial \tau_i$ may be equal to zero for one or more i.

As an example, we consider a second-order system described by

$$\begin{bmatrix}\dot{x}_1 \\ \dot{x}_2\end{bmatrix} = \begin{bmatrix}0 & 1 \\ -a_1 & -a_2\end{bmatrix}\begin{bmatrix}x_1 \\ x_2\end{bmatrix} + \begin{bmatrix}0 \\ f_1(x_1) + f_2(x_2)\end{bmatrix} + \begin{bmatrix}0 \\ v_1(x_1) + b\end{bmatrix} u(t) \tag{25}$$

where f_1, f_2, and v_1 are unknown Lipshitz continuous functions with continuous derivatives. We identify a nominal linear system $\mathbf{z}$ consisting only of the linear portions of (25), with the $\mathbf{z}$ and $\mathbf{x}$ dynamics differing by bounded nonlinearities

$$|f_1(x_1)| \leq \delta_1|x_1|, |f_2(x_2)| \leq \delta_2|x_2|, |\nu_1(x_1)| \leq \delta_u|x_1|$$
$$\left|\frac{df_1(x_1)}{dx_1}\right| \leq \delta_1', \left|\frac{df_2(x_2)}{dx_2}\right| \leq \delta_2', \left|\frac{d\nu_1(x_1)}{dx_1}\right| \leq \delta_u'. \tag{26}$$

Then, as $z(t)$ may be solved for a given $u(t)$, bounds on the difference between $\mathbf{x}$ and $\mathbf{z}$ may be obtained from

$$\frac{d}{dt}\begin{bmatrix}|x_1-z_1|\\|x_2-z_2|\end{bmatrix} \le \begin{bmatrix}|x_2-z_2|\\(|a_1|+\delta_1'+\delta_u'u)|x_1-z_1|+(|a_2|+\delta_2')|x_2-z_2|\end{bmatrix} + \begin{bmatrix}0\\(\delta_1+\delta_u u)|z_1|+\delta_2|z_2|\end{bmatrix}. \tag{27}$$

Derivatives of ψ with respect to initial conditions may likewise be bounded. By [30], these derivatives are known to be solutions to the set of differential equations

$$\begin{aligned}
\frac{d}{dt}\left(\frac{\partial\psi_{i,1}}{\partial x_1(0)}\right)&=\frac{\partial\psi_{i,2}}{\partial x_1(0)}\\
\frac{d}{dt}\left(\frac{\partial\psi_{i,1}}{\partial x_2(0)}\right)&=\frac{\partial\psi_{i,2}}{\partial x_2(0)}\\
\frac{d}{dt}\left(\frac{\partial\psi_{i,2}}{\partial x_1(0)}\right)&=\left(-a_1+\frac{df_1(x_1)}{dx_1}+\frac{dv_1(x_1)}{dx_1}u_{\max}\cdot i\right)\\
&\quad\times\left(\frac{\partial\psi_{i,1}}{\partial x_1(0)}\right)+\left(-a_2+\frac{df_2(x_2)}{dx_2}\right)\left(\frac{\partial\psi_{i,2}}{\partial x_1(0)}\right)\\
\frac{d}{dt}\left(\frac{\partial\psi_{i,2}}{\partial x_2(0)}\right)&=\left(-a_1+\frac{df_1(x_1)}{dx_1}+\frac{dv_1(x_1)}{dx_1}u_{\max}\cdot i\right)\\
&\quad\times\left(\frac{\partial\psi_{i,1}}{\partial x_2(0)}\right)+\left(-a_2+\frac{df_2(x_2)}{dx_2}\right)\left(\frac{\partial\psi_{i,2}}{\partial x_2(0)}\right)
\end{aligned} \tag{28}$$

with initial conditions $\partial\psi_{i,1}/\partial x_1(0)=1$, $\partial\psi_{i,1}/\partial x_2(0)=0$, $\partial\psi_{i,2}/\partial x_1(0)=0$, and $\partial\psi_{i,2}/\partial x_2(0)=1$, where $i=(0,1)$ corresponding to "ON" and "OFF" responses, as before, and $\psi_{i,1}$ and $\psi_{i,2}$ referring to the first and second states in either case.

The equations in (28) become a pair of second-order differential equations that may be bounded, as in (27), where $\mathbf{z}_a=[z_{a1}(t)z_{a2}(t)]^{\mathrm{T}}$ and $\mathbf{z}_b=[z_{b1}(t)z_{b2}(t)]^{\mathrm{T}}$ are solutions to the linear portions of (25) with initial conditions [1 0] and [0 1], respectively, and zero input.

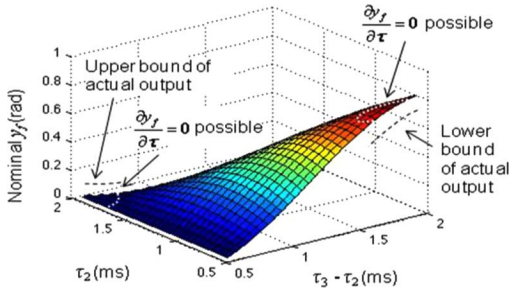

Fig. 4. Nominal system output as a function of switching times τ_2 and τ_3 for $p=3$, $\tau_1=0.5$ ms, and $u_{\max}=20$, and marked regions of possible local minima/maxima when unknown, bounded nonlinearities are present.

By finding nominal responses $\mathbf{z}, \mathbf{z}_a$, and $\mathbf{z}_b$, and solving for bounds between them and true system responses as a function of time using (27) and (29) (shown at the bottom of the page), ranges of possible $\partial y_f/\partial\tau_i$ values may finally be found, as for τ_p, shown in (30) at the bottom of the page.

In relationships the z terms may be known exactly, while the quantities in braces may be bounded using (28), allowing evaluation of $\partial y_f/\partial\tau_p=0$ feasibility.

Fig. 4 shows the output of the nominal system (26) as a function of switching times τ_2 and τ_3 when $\tau_1=0.5$ ms and $p=3$. Nonlinearity bounds are given in Table I, representing the experimental system in the following Section, where natural frequency (related to a_1) and gain estimates (related to b) are quite accurate, but there may be substantial error in damping estimates (related to a_2). While $\partial y_f/\partial\tau_2=0$ and $\partial y_f/\partial\tau_3=0$ do not quite occur for the nominal system with this τ_1, when uncertainty in the derivatives due to nonlinearities is accounted for, locations, where $\partial y_f/\partial\tau_2=0$ and $\partial y_f/\partial\tau_3=0$ become

$$\frac{d}{dt}\begin{bmatrix}\left|\frac{\partial\psi_{i,1}}{\partial x_1(0)}-z_{a1}\right|\\\left|\frac{\partial\psi_{i,1}}{\partial x_2(0)}-z_{b1}\right|\\\left|\frac{\partial\psi_{i,2}}{\partial x_1(0)}-z_{a2}\right|\\\left|\frac{\partial\psi_{i,2}}{\partial x_2(0)}-z_{b2}\right|\end{bmatrix} \le \begin{bmatrix}\left|\frac{\partial\psi_{i,2}}{\partial x_1(0)}-z_{a2}\right|\\\left|\frac{\partial\psi_{i,2}}{\partial x_2(0)}-z_{b2}\right|\\(|a_1|+\delta_1')\left|\frac{\partial\psi_{i,1}}{\partial x_1(0)}-z_{a1}\right|+(|a_2|+\delta_2')\left|\frac{\partial\psi_{i,2}}{\partial x_1(0)}-z_{a2}\right|\\(|a_1|+\delta_1')\left|\frac{\partial\psi_{i,1}}{\partial x_2(0)}-z_{b1}\right|+(|a_2|+\delta_2')\left|\frac{\partial\psi_{i,2}}{\partial x_2(0)}-z_{b2}\right|\end{bmatrix} + \begin{bmatrix}0\\0\\(\delta_1'+\delta_u'u_{\max}\cdot i)|z_{a1}|+\delta_2'|z_{a2}|\\(\delta_1'+\delta_u'u_{\max}\cdot i)|z_{b1}|+\delta_2'|z_{b2}|\end{bmatrix} \tag{29}$$

$$\begin{aligned}
\frac{\partial y_f}{\partial\tau_p}&=[-z_2(t_f)-\{x_2(t_f)-z_2(t_f)\}]\\
&\quad+\left[z_{a1}(t_f-\tau_p)+\left\{\frac{\partial\psi_{0,1}}{\partial x_1(0)}-z_{a1}(t_f-\tau_p)\right\}\right][z_2(\tau_p)+\{x_2(\tau_p)-z_2(\tau_p)\}]\\
&\quad+\left[z_{b1}(t_f-\tau_p)+\left\{\frac{\partial\psi_{0,1}}{\partial x_2(0)}-z_{b1}(t_f-\tau_p)\right\}\right]\\
&\quad\cdot\begin{bmatrix}-a_1(z_1(\tau_p)+\{x_1(\tau_p)-z_1(\tau_p)\})-a_2(z_2(\tau_p)+\{x_2(\tau_p)-z_2(\tau_p)\})\\+f_1(z_1(\tau_p)+\{x_1(\tau_p)-z_1(\tau_p)\})+f_2(z_2(\tau_p)+\{x_2(\tau_p)-z_2(\tau_p)\})+v_1(z_1(\tau_p)+\{x_1(\tau_p)-z_1(\tau_p)\})\end{bmatrix}
\end{aligned} \tag{30}$$

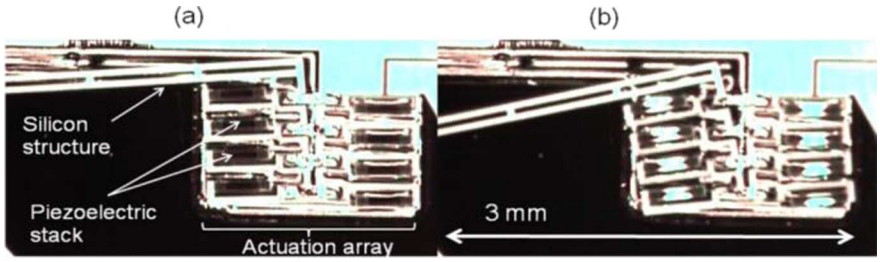

Fig. 5. Sample image of the MEMS leg actuator.

TABLE I
NOMINAL SYSTEM COEFFICIENTS AND BOUNDS ON CORRESPONDING NONLINEARITIES DEVIATING FROM THESE COEFFICIENTS

	Value	Non-linearity	Bound $\delta_{(.)}$	Bound $\delta'_{(.)}$
a_1	$3.06{\cdot}10^6$ s^{-2}	$f_1(x_1)$	$6.1{\cdot}10^4$ s^{-2}/rad	$2.5{\cdot}10^5$ s^{-2}/rad
a_2	51 s^{-1}	$f_2(x_1)$	10 s^{-1}/(rad/s)	40 s^{-1}/(rad/s)
b	$6.9{\cdot}10^6$ s^{-2}/V	$v_u(x_1)$	$1.4{\cdot}10^3$ s^{-2}/V/rad	$5.5{\cdot}10^3$ s^{-2}/V/rad

possible and are outlined in white (with no distinction at present for local minima versus maxima). In addition, possible response variation is marked, indicating that the worst case system outputs for the points, where $\partial y_f/\partial\tau_2 = 0$ and $\partial y_f/\partial\tau_3 = 0$ may be true are below 0.15 rad and above 0.42 rad. Taking into account $\partial y_f/\partial\tau_1$ as well, we ultimately conclude that the range of outputs between 0.12 and 0.43 rad are free of local minima, and that selecting initial switching times according to $0.1 < \tau_1 < 0.8$ ms, $1 < \tau_2 < 1.4$ ms, and $1.6 < \tau_3 < 1.8$ ms should be sufficient to reach target outputs between 0.12 and 0.42 rad.

VI. EXPERIMENTAL EXAMPLE

A. Experimental Setup

An MEMS multiactuator leg joint was used to verify behavior under the proposed controller. Fig. 5 shows the leg joint tested. Several thin-film piezoelectric actuators compose this leg with a natural frequency of approximately 279 Hz and a nominal damping ratio 0.017.

The experimental system with the input range 0–20 V, modeled as a second-order linear system has a nominal linear model, as shown in Fig. 6, of

$$\begin{bmatrix}\dot{z}_1\\ \dot{z}_2\end{bmatrix} = \begin{bmatrix}0 & 1\\ -3.06e^6 & -51\end{bmatrix}\begin{bmatrix}z_1\\ z_2\end{bmatrix} + \begin{bmatrix}0\\ 6.9e^5\end{bmatrix}u(t). \quad (31)$$

Leg motion was measured by filming the microscale leg through a stereoscope using a high-speed camera system. Images were collected at 4000 fps, and angle measurements in each frame were extracted using the MATLAB Image Processing Toolbox; off-board sensing was used because, although integrated sensing has been implemented on other types of piezoelectric actuators on the test wafer, the current robotic leg prototypes are not yet instrumented with these sensors. Image measurement error was interpreted as noise, and estimated at $\tilde{\varepsilon} = N(0, 0.01^2)$ as its influence on the cost function. The control signal is generated on a control circuitry, which was

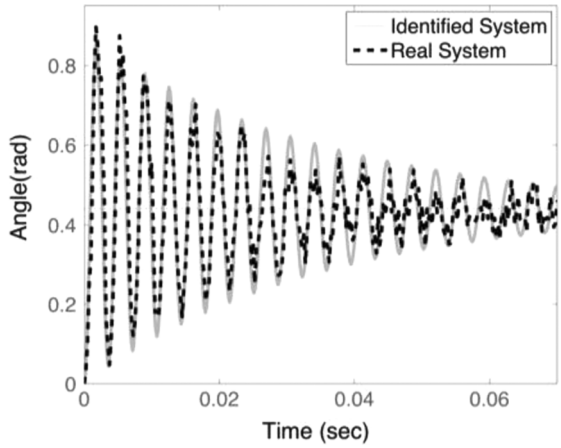

Fig. 6. Step response and nominal linear dynamics of the experimental system.

implemented with an off-board TMS320F28335 DSP and a level shifter circuit based on CMOS inverter [29] acting as the ON–OFF interface between the low-voltage DSP and a 20 V supply $(u_{\max})$ for the actuator.

B. Experimental Results

Various target motions were tested to verify controller performance. Two sample reference levels $r = 0.2$ rad and $r = 0.3$ rad, where a value of 0.45 rad corresponds to the maximum static actuator displacement, are shown in Fig. 7. In both cases, $p = 3$ for vector τ, and the final time t_f was 2 msec. Initial guesses for switching times were selected based on the convergence analysis as [0.7 ms 1.1 ms 0.17 ms]. The CPU operation time was 0.05 msec. The experimental controller uses only one measured value at the final time t_f. Selected gain coefficients values of a, c, A, α, and γ were $0.0016, 5e^{-5}, 200, 0.602$, and 0.101, respectively, based on rules of Section IV-C.

Fig. 7(a) and (b) shows sample experimental responses with obtained optimal τ of [0.7 ms 1.1 ms 1.2 ms]^T and [0.6 msec 1.1 ms 1.21 ms]^T for $r = 0.3$ rad and $r = 0.2$ rad, respectively. The experimental results show a successful convergence to the target reference level as and in just two to three iterations or two iterations. While a true gradiant-based search is expected to be faster, if full model information were available [11], this is a rapid convergent rate when tens or hundreds of repeated motions are needed, as in a microrobotic walking gait. Energy consumed by the actuator during a single iteration is just 0.9 μJ. While off-board sensing was used for the experimental verification performed here, a single measurement taken from a capacitive sensor once for every cycle, in which the actuator has

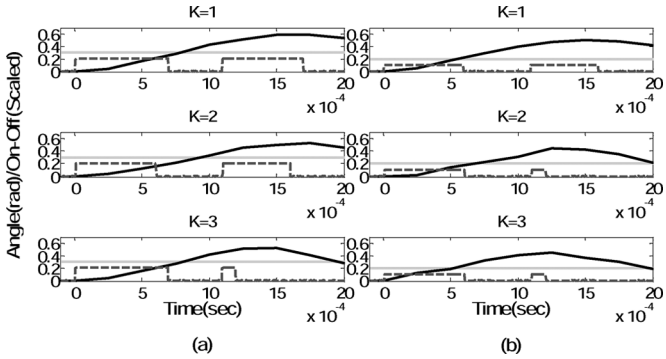

Fig. 7. Experimental results for the system (31): (a) for reference 0.3 rad and (b) for reference 0.2 rad (black line: output; gray dashed line: input; and gray line: target).

been allowed to move and then return to its original position, would require sampling at approximately 14 times per second. This would correspond to energy consumption of less than 0.8μJ for each iteration using state-of-the-art sensing circuitry. Anticipated power consumption for the entire system would then be about 24 μW.

VII. Discussion and Conclusion

The strength of the proposed controller for regulating microsystem motion is that it relies on extremely simple sensing and input capabilities, which allows it to perform control at very low power. Typically, good performance is observed by the authors when using just a few more switching transitions than the order of the target system. The use of a well-established gradient estimation algorithm allows the designer to be confident of convergence of the iterated response to a minimal value of the cost function presented, although greater effort is required to provide confidence in achieving a true global minimum. This does not guarantee a specified convergence rate, but in all experimental and simulation tests performed by the authors, convergence rate has been quite fast, requiring between 3 and 15 iterations. Increasing the number of switching times may reduce the likelihood of $\partial y_f/\partial \tau_i = 0$ for all switching times, without a substantial reduction in convergence rate, but with an increase in power consumption by a capacitive load. No model of the system is required by the controller, reducing memory and modeling.

There are major limitations of the control algorithm as well. Because the controller only assesses motion at one point each iteration, it cannot be used to hold the system output at its target beyond the final time; its usefulness to microrobotics, for instance, is tied to the ability to switch motion to another leg when one actuator is finished moving. In addition, identifying possible locations of local minima becomes extremely cumbersome as the number of switching transitions and/or system order increases, and the error bounds used in the procedure in Section V rapidly increase with time. As a result, the controller remains most predictable for low-order systems undergoing transient motions over a fixed time period, and is useful when ultralow power consumption is critical.

To conclude, we have described a method for implementing model-free adaptive ON–OFF control through the application of SPSA. This control technique can be very useful in control of repeated motions by systems with extremely limited power budgets, where power consumption at sensor measurements and in analog drive circuitry is to be avoided. The controller presented can be implemented with just a single sensor measurement per iteration, and has been observed to result in rapid convergence to a desired final output. Such a controller may ultimately be used to help regulate leg motions in the walking gait of a piezoelectrically actuated terrestrial microrobot.

Acknowledgment

The authors would like to thank the Army Research Laboratory for the prototype robotic leg joint used in experimental testing.

References

[1] J. A. Main, "Efficient power amplifiers for piezoelectric applications," *Smart Mater. Struct.*, vol. 5, no. 6, pp. 766–775, 1996.

[2] W. Bracke, P. Merkin, R. Puers, and C. Van Hoof, "Ultra-low-power interface chip for autonomous capacitive sensor systems," *Circuits Syst. I, Reg. Papers*, vol. 54, no. 1, pp. 130–140, Jan. 2007.

[3] C. Y. Kaya and J. L. Noakes, "Computations and time-optimal controls," *Optimal Control Appl. Methods*, vol. 17, pp. 171–185, 1996.

[4] B. Edamana and K. Oldham, "An optimal on-off controller with switching costs using non-linear binary programming ," in *Proc. Amer. Control Conf.*, 2009, pp. 4227–4232.

[5] K. Oldham, B. Hahn, B. Edamana, J. Pulskamp, and R. Polcawich, "Low-power switching control schemes for piezoelectric micro-robotic actuators," presented at the ASME Conf. Smart Mater., Adaptive Structures Intell. Syst., Ellicot City, MD, 2008.

[6] W. C. West, J. F. Whitacre, E. J. Brandon, and B. V. Ratnakumar, "Lithium micro-battery development at the jet propulsion laboratory," *IEEE Aerosp. Electron. Syst. Mag.*, vol. 16, no. 8, pp. 31–33, Aug. 2001.

[7] J. L. Noakes and C. Y. Kaya, "Computational method for time-optimal switching control," *J. Optim. Theory Appl.*, vol. 117, no. 1, pp. 69–92, 2003.

[8] D. G. Luenberger, *Linear and Nonlinear Programming*. Reading, MA: Addison-Wesley, 1989 .

[9] S. K. Lucas and C. Y. Kaya, "Switching-time computation for bang-bang control laws," in *Proc. Amer. Control Conf.*, 2001, pp. 176–179.

[10] J. C. Spall, "Multivariate stochastic approximation using a simultaneous perturbation gradient approximation ," *IEEE Trans. Autom. Control*, vol. 37, no. 3, pp. 332–341, Mar. 1992.

[11] J. C. Spall, "An overview of the simultaneous perturbation method for efficient optimization," *J. Hopkins APL Tech. Dig.*, vol. 19, no. 4, pp. 482–492, 1998.

[12] J. C. Spall, "A one-measurement form of simultaneous perturbation stochastic approximation," *Automatica*, vol. 33, no. 1, pp. 109–112, 1997.

[13] J. C. Spall, "Implementation of the simultaneous perturbation algorithm for stochastic optimization ," *IEEE Trans. Aerosp. Electron. Syst.*, vol. 43, no. 3, pp. 817–823, Jul. 1998.

[14] P. Sadegh and J. C. Spall, "Optimal random perturbation for stochastic approximation using simultaneous perturbation gradient approximation," *IEEE Trans. Autom. Control*, vol. 43, no. 10, pp. 1480–1484, Oct. 1998.

[15] F. Rezayat, "On the use of an SPSA-based model-free controller in quality improvement," *Automatica*, vol. 31, no. 6, pp. 913–915, 1995.

[16] J. C. Spall, "Model-free control of nonlinear stochastic systems with discrete-time measurements," *IEEE Trans. Autom. Control*, vol. 43, no. 9, pp. 1198–1210, Sep. 1998.

[17] V. Aksakalli and D. Ursu, "Control of nonlinear stochastic systems: Model-free controllers versus linear quadratic regulators ," in *Proc. 45th IEEE Conf. Dec. Control*, 2006, pp. 4145–4150.

[18] Q. Zhang, Y. Zhou, X. Liu, X. Li, and W. Gan, "A nonlinear ANC system with a SPSA-based recurrent fuzzy neural network controller," in *Proc. 4th Int. Symp. Neural Netw.*, 2007, pp. 176–182.

[19] K. Oldham, J. S. Pulskamp, R. G. Polcawich, and M. Dubey, "Thin-film PZT lateral actuators with extended stroke," *J. MEMS*, vol. 17, no. 4, pp. 890–899, 2008.

[20] L. H. Ragan, "Radio receiver with adaptive on-off control," U.S. Patent 5 155 479, Oct. 13, 1992.

[21] P. V. Zhivoglyadov, R. H. Middeton, and M. Fu, "Localization based switching adaptive control for time-varying discrete-time systems ," *IEEE Trans. Autom. Control*, vol. 45, no. 4, pp. 752–755, Apr. 2000.

[22] C.-H. Wang, T.-C. In, T.-T. Lee, and H.-L. Liu, "Adaptive hybrid intelligent control for uncertain nonlinear dynamical systems," *IEEE Trans. Syst., Man Cybern.*, vol. 32, no. 5, pp. 583–587, Oct. 2002.

[23] S. N. Huang, K. K. Tan, and T. H. Lee, "Nonlinear adaptive control of interconnected systems using neural networks," *IEEE Trans. Neural Netw.*, vol. 17, no. 1, pp. 243–246, Jan. 2006.

[24] T. H. Hayakawa, W. M. Haddad, and N. Hovakimyan, "Neural network adaptive control for a class of nonlinear uncertain dynamical systems with asymptotic stability guarantees," *IEEE Trans. Neural Netw.*, vol. 19, no. 1, pp. 80–89, Jan. 2008.

[25] J.-C. Fort and G. Pages, "Convergence of stochastic algorithms: From the Kushner-Clark theorem to the Lyapounov functional method," *Adv. Appl. Prob.*, vol. 28, no. 4, pp. 1072–1094, 1996.

[26] L. Ljung, "Analysis of recursive stochastic algorithms," *IEEE Trans. Autom. Control*, vol. AC-22, no. 4, pp. 551–575, Aug. 1977.

[27] P. Sadegh, "Constrained optimization via stochastic approximation with a simultaneous perturbation gradient approximation," *Automatica*, vol. 33, no. 5, pp. 889–892, 1997.

[28] D. C. Chin, "Comparative study of stochastic algorithms for system optimization based on gradient approximations ," *IEEE Trans. Syst., Man, Cybern.*, vol. 27, no. 2, pp. 244–249, Apr. 1997.

[29] B. Edamana, B. Hahn, J. S. Pulskamp, R. G. Polcawich, and K. Oldham, "Modeling and optimal low-power on-off control of thin-film piezoelectric actuators," *IEEE/ASME Trans. Mechatron.*, to be published.

[30] T. H. Gronwall, "Note on the derivatives with respect to a parameter of a system of differential equations ," *Ann. Mater.*, vol. 20, pp. 292–296, 1919.